

Morphology and thermal behaviour of poly(methyl methacrylate) /poly(ethylene glycol) /multi-walled carbon nanotubes nanocomposites

G. Q. Liu*

College of Material Science and Engineering, Henan University of Technology, Zhengzhou, 450001, China.

Received December 25, 2013, Revised July 3, 2015

Poly(methyl methacrylate) /poly(ethylene glycol) /multi-walled carbon nanotubes (PMMA/PEG/MWNTs) nanocomposites were prepared by ultrasonic assisted free radical bulk polymerization. The effect of different weight percent loadings of MWNTs on the morphological and thermal properties of PMMA/PEG/MWNTs nanocomposites had been investigated. It was found that, at low concentration of MWNTs, it could uniformly disperse into PMMA/PEG blends and increase the nucleation density of PEG. Thermal analysis showed that a clear improvement of thermal stability for PMMA/PEG/MWNTs nanocomposites increased with increasing MWNTs content.

Keywords: PMMA, PEG, MWNTs, morphology, thermal behaviour

INTRODUCTION

Polymer nanocomposites with lower nanofiller's loading display more superior properties than conventional composites, and have increasingly drawn attention because of their many advantages such as flexible features, easy processing, and lightweight [1-9], especially polymers/carbon nanotubes (CNTs) nanocomposites [10-13]. CNTs are ideal fillers for polymer nanocomposites and have high Young modulus, tensile strength, good electrical conductivity and thermal conductivity, together with the need for only small volume fractions to obtain desired properties; therefore, polymers/CNTs nanocomposites could use for the development of advanced multifunction materials [14-16].

Generally, CNTs can consist of single-walled carbon nanotubes (SWNTs) and multi-walled carbon nanotubes (MWNTs). They can be prepared by three techniques: laser ablation, arc discharge and chemical vapour decomposition (CVD) [17]. Among them, CVD is the most commonly used method for mass production of different types of CNTs. Although SWNTs offer the opportunity for much lower loading versus MWNTs to achieve the same electrical properties, enhancing mechanical properties even further [18], MWNTs are widely used as a result of lower unit cost, greater availability and fewer dispersion challenges compared with SWNTs.

Linear poly(methyl methacrylate) (PMMA) can form stable blends with linear poly(ethylene oxide) (PEO) due to van der Waals type bonding between the PMMA chains and the planar PEO segments

[19-21], which is among the most studied polymer systems; however, its relatively poor heat resistance hinders specific applications; therefore, many studies are reported in the literature concerning PMMA nanocomposites [22-27]. In this work, to enhance and utilize the properties of PMMA/PEG, especially to improve heat resistance, PMMA/PEG/MWNTs nanocomposites were prepared by ultrasonic assisted free radical bulk polymerization. The effects of MWNTs on the morphology, crystal structure and thermal stability of PMMA/PEG/MWNTs nanocomposites were investigated. This paper is aimed at presenting the fabrication methods of nanocomposites and the CNTs-modified properties of polymer.

EXPERIMENTAL

Material

MWNTs were purchased from Shenzhen Nano-Technologies Port Co. Ltd., China, with a purity of above 96 %, average length of microns, and surface area of $4.26 \text{ m}^2 \cdot \text{g}^{-1}$. Methyl methacrylate (MMA) and azobisisobutyronitrile (AIBN) were of analytical grade obtained from the Chengdu Reagent Factory. Ethylene glycol dimethacrylate (EGDMA) was purchased from Aldrich Chemical Co. MMA was distilled under reduced pressure before use. AIBN, used as a radical initiator, was recrystallized from methanol solution. EGDMA was used as a cross-linker without further purification. Polyethylene glycol (PEG, Aldrich, $M_n=2000$) was dried by heating at $70 \text{ }^\circ\text{C}$ for 7 hrs under vacuum, which also played a role of an organic dispersant.

* To whom all correspondence should be sent:
E-mail: mikepolymer@126.com

Preparation of PMMA/PEG/MWNTs nanocomposites

Firstly, MWNTs were immersed in 3 mol·l⁻¹ nitric acid (HNO₃) and refluxed for 8 hrs, subsequently washed with distilled water until the pH of MWNTs solution was ca. 7, finally obtained after dried in a vacuum oven at 90 °C for 40 hrs. Adding the gained MWNTs (0.5-3 wt.%), MMA (54.5-57 wt.%) and PEG (38 wt.%) into a two-necked flask, the mixtures was sonicated using a bath sonicator for 1 hr. AIBN (1 wt.%) as an initiator, and EGDMA (3.5 wt.%) as a crosslinker, were added and nitrogen gas was purged into the flask to remove oxygen. Polymerization was carried out with constant stirring at 60 °C for 10 min. Then, the reaction mixture injected into the space between two glass plates separated by polyethylene spacers (3 mm thick) and continued to polymerize by ultrasonic assisting at 55 °C for 24 hrs. The prepared PMMA/PEG/MWNTs nanocomposites were quenched and then dried under vacuum at room temperature for 72 hrs to remove unreacted monomers.

Characterizations

MWNTs size analysis was performed on a Microtrac S3000 analyzer (Microtrac Software Co., USA). The spherulitic morphology was observed and photographed through a polarized optical microscope (POM, a Jiangnan XPR-2, China) equipped with a digital camera. Thermogravimetric analysis (TGA) measurement was performed using TGA-7 (Perkin-Elmer). The thermal analyses were carried out with a differential scanning calorimeter (DSC, DuPont 9900) over a temperature range from -70 to 155 °C at a heating rate of 10 °C·min⁻¹, purged with nitrogen gas, and quenched with liquid nitrogen. The cell was calibrated using an indium standard; the weight of the sample was 5-10 mg. SEM observation was carried out with a JSM-5900LV scanning electron microscopy. TEM measurements were carried out on a FEI Fecnai F20 S-Twin transmission electron microscope, operating at an accelerating voltage of 200 kV.

RESULTS AND DISCUSSION

It is well known that the dispersion of CNTs in the polymer matrix and their interfacial interactions are the key factors to ultimately determine many properties of polymers/CNTs nanocomposites, including improving the mechanical, electrical, and thermal performances of the polymer matrix. The TEM image of as as-received MWNTs is shown in Fig.1 (a) and their diameter distribution is measured, as shown in Fig.1 (b). The specifications

of MWCNTs are as follows: 93 % MWNTs smaller than 100 nm with average diameters = 68 nm, and about 0.8 % larger than 200 nm.

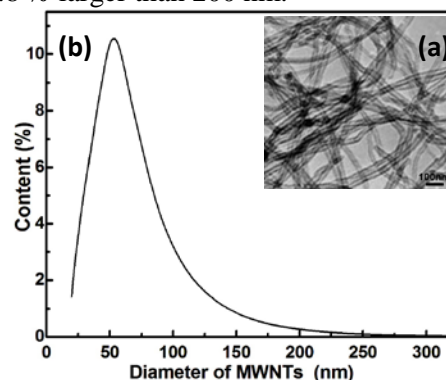


Fig. 1. TEM image (a) and distribution of diameter (b) for as-received MWNTs.

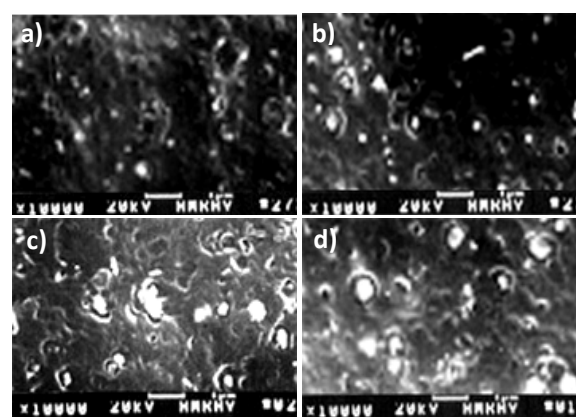


Fig. 2. SEM images of PMMA/PEG/MWNTs nanocomposites. a) PMMA/PEG/0.5 wt.% MWNTs, b) PMMA/PEG/1 wt.% MWNTs, c) PMMA/PEG/2 wt.% MWNTs, d) PMMA/PEG/3.0 wt.% MWNTs.

To reveal dispersion of MWNTs in the PMMA/PEG blends, the cryo-fractured surfaces of the nanocomposites were investigated in detail by SEM, as shown in Fig. 2 a) - d). A fibrous fractured surface is observed due to the elongation at break of PMMA/PEG/MWNTs nanocomposites; the random dispersed bright dots because of MWNTs high conductivity are the ends of the broken carbon nanotubes [28]. In addition, it is found that some MWNTs are broken apart, and, as a result of poor interfacial adhesion, some MWNTs are pulled out of the matrix before the breakage, forming caves on the fractured surface; moreover, other MWNTs are observed with their one end still strongly embedded in the PMMA/PEG blends as an inset. Such interesting and typical breakage phenomenon of the MWNTs indicates that a strong interfacial adhesion exists between MWNTs and PMMA/PEG blends and that the load transfer takes place efficiently from the matrix to the nanotubes. The strong is usually responsible for the significant enhancement of the mechanical properties [29]. This interfacial

adhesion may be ascribed to the following facts: carboxylic acid groups could be formed at the open ends and at defect sides of the side walls of CNTs after the strong acid treatment [30, 31], therefore, the hydrogen bonds could exist in between the PEG hydroxyl group and the carbonyl group of MWNTs, which would help to disperse MWNTs in PMMA/PEG/MWNTs nanocomposites.

At low concentration of MWNTs, from Fig. 2 a) and 2 b), it can be seen that the bright dots (i.e., MWNTs) embedded in the PMMA/PEG blends and the caves (i.e., MWNTs) pulled out from the PMMA/PEG blends are well dispersed; however, with an increase in MWNTs concentration, from Fig. 2 c) and 2 d), a nonuniform dispersion of MWNTs is observed in the nanocomposites, and a large aggregate of MWNTs having a diameter of over 500 nm is presented; while in the case of pristine MWNTs, its diameter is about 70 nm, as shown in Fig. 1. Those indicate that the MWNTs were dispersed as nanotubes aggregates due to the imperfect mixing of the masterbatch.

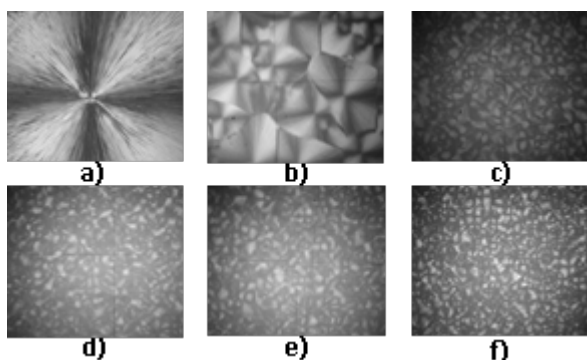


Fig. 3. Spherulitic morphologies of a) neat PEG2000, b) PMMA/PEG2000, c) PMMA/PEG2000/0.5 wt.% MWNTs, d) PMMA/PEG/1 wt.% MWNTs, e) PMMA/PEG/2 wt.% MWNTs, and f) PMMA/PEG/3.0 wt.% MWNTs crystallized at 0 °C by POM ($\times 20$).

When the content of MWNTs is no more than 1.0 wt.%, owing to producing carboxylic or hydroxylic groups on the surface of the MWNT, which ensures the high dispersion quality of the MWNTs and prevents the severe aggregation of MWNTs [32, 33], reasonably uniform distribution of the MWNTs is observed in Fig. 2 a) and 2 b). On the other hand, at compositions containing greater amounts of MWNTs, a small amount of aggregates is shown in Fig. 2 c) and 2 d). These results are in good agreement with the results of Wu et al. and Bikiaris et al. who reported that increasing the content of SiO₂ leads to larger agglomerates [34, 35]; this is also the case in PMMA/PEG/MWNTs nanocomposites. In fact, there are more or less agglomerates of MWNTs formed in Fig. 2.

The effect of MWNTs on the spherulitic morphology of PEG blends was studied by POM. Fig. 3 shows the spherulitic morphology of neat PEG2000, PMMA/PEG blends and PMMA/PEG/MWNTs nanocomposites crystallized at 0 °C. Well-developed spherulite grows to a size of about 2000 μm in diameter in the case of neat PEG2000, as shown in Fig. 3 a). Spherulites are the basic morphology for polymers crystallized from melting or concentrated solutions, which are high-order crystal structures with spherical textures composed of lamellar crystallites shaped like ribbons that radiate from the center, separated by amorphous material [16]. For the PMMA/PEG blends, as shown in Fig. 3 b), it is clear that the presence of PMMA networks limited the PEG spherulites growth. Parts c), d), e), and f) of Fig. 3 illustrate the POM images of PEG spherulites after nanocomposites preparation with MWNTs. It is clear that the size of PEG spherulites becomes smaller in the presence of MWNTs, indicative of the increase of nucleation density; some smaller and imperfect spherulites with diameter less than 200 μm are observed to grow rapidly, impinge quickly with surrounding spherulites, and restrict further growth. Spherulitic morphology studies indicate that the nucleation density of PEG is improved due to the presence of MWNTs in the nanocomposites and MWNTs seem very effective as a nucleation agent.

It is of great interest to study the effect of the incorporation of MWNTs on the crystal structure of PEG in the nanocomposites. Fig. 4 illustrates the WAXD patterns of neat PEG2000 and PMMA/PEG/MWNTs nanocomposites, which were crystallized at 0 °C for 12 hrs.

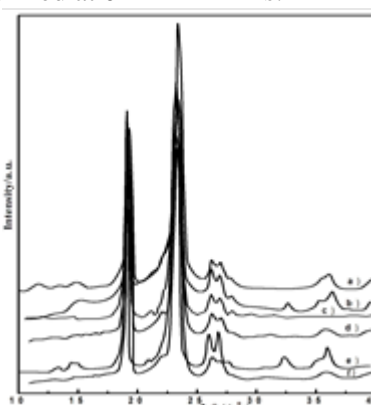


Fig. 4. WAXD patterns of a) neat PEG2000, b) PMMA/PEG2000, c) PMMA/PEG2000/0.5 wt.% MWNTs, d) PMMA/PEG2000/1 wt.% MWNTs, e) PMMA/PEG2000/2 wt. % MWNTs, f) PMMA/PEG2000/3 wt. % MWNTs.

It should be noted that PEG2000 and PMMA/PEG/MWNTs nanocomposites have

similar diffraction patterns, and so are their diffraction angles and crystal plane distances. Neat PEG2000 shows two main diffraction peaks at about 18.9° and 23.1°, whose positions don't change in PMMA/PEG/MWNTs nanocomposites, which demonstrates that neat PEG2000 and PMMA/PEG/MWNTs nanocomposites have similar crystal structure and crystal cell type, and there are no significant distortions of the crystal structures of PEG in nanocomposites. In other words, the crystal structure of PEG has not been changed by the procedure of blending, and therefore, there are no chemical changes at all. The main difference between neat PEG2000 and PMMA/PEG/MWNTs nanocomposites is that the diffraction peak height and half-width of the former are lower and narrower than those of the latter, which means that the dimension of spherulites becomes smaller and the degree of crystallization decreases; the result is consistent with POM results.

It is of great interest to study the melting behavior of neat PEG2000, PMMA/PEG2000 and its nanocomposites because crystal structures and crystallinity play significant roles in the mechanical and other properties of crystalline polymers. DSC analysis is a generally convenient method for analyzing first order transitions like melting.

Fig. 5 shows the thermal diagram measured during heating.

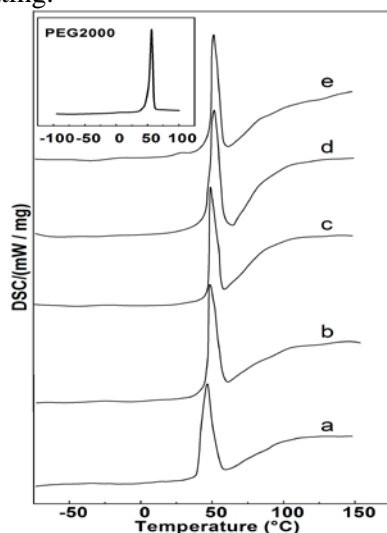


Fig. 5. DSC scans of neat PEG2000, PMMA/PEG2000 (a), PMMA/PEG2000/0.5 wt.% MWNTs (b), PMMA/PEG2000/1 wt.% MWNTs (c), PMMA/PEG2000/2 wt.% MWNTs (d), and PMMA/PEG2000/3 wt.% MWNTs (e).

The PMMA/PEG/MWNTs nanocomposites possess a melting endothermic peak (T_m) during heating; it can be observed that T_m increase slightly in the PMMA/PEG/MWNTs nanocomposite compared with those in PMMA/PEG blend, and increase with increase of MWNTs concentration, as

shown in Table 1, which indicates that the MWNTs presence does not prevent PEG crystallization, and act as an nucleation reagent for the PEG crystallization; meanwhile, the melting enthalpy (ΔH_m) which are determined from the area under the endotherm, are increased in the nanocomposites as compared with that of PMMA/PEG blend in Table 1. The weight crystallinity indexes (X_c) of the PEG phase, PMMA/PEG2000 and PMMA/PEG2000/MWNTs nanocomposites are calculated from:

$$X_c = \Delta H_m / \Delta H_{PEG}^{\circ} \quad (1)$$

Where ΔH_{PEG}° is the heat of fusion per gram of 100 % crystalline PEG (from literature data [36], $\Delta H_{PEG}^{\circ} = 45 \text{ cal}\cdot\text{g}^{-1}$).

Table 1. DSC results for PEG2000, PMMA/PEG2000 and its nanocomposites.

Sample	T_m (°C)	ΔH_m (J/g)	X_c (%)
PEG2000	57	178	94
PMMA/PEG2000	46.5	26.5	14
PMMA/PEG2000/0.5 wt% MWNTs	48.6	30.2	16
PMMA/PEG2000/1.0 wt% MWNTs	49.7	32.3	17
PMMA/PEG2000/2.0 wt% MWNTs	50.8	34.1	18
PMMA/PEG2000/3.0 wt% MWNTs	51.7	35.9	19

Although X_c of PMMA/PEG2000 and PMMA/PEG2000/MWNTs nanocomposites are much lower than that of pure PEG2000, they increase with increasing of MWNTs content for PMMA/PEG2000/MWNTs nanocomposites. From above results, compared to PMMA/PEG blends, it can be concluded that the incorporation of MWNTs enhances the crystallization of PEG2000 in the nanocomposites, which should be attributed to the strong heterogeneous nucleation of MWNTs [26].

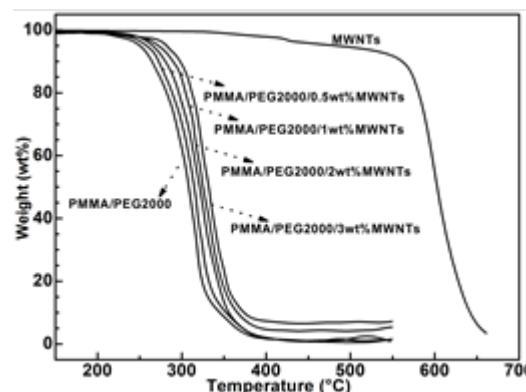


Fig. 6. TGA curves of MWNTs, PMMA/PEG2000 and PMMA/PEG2000/MWNTs nanocomposites.

Fig. 6 shows TGA thermograms of PMMA/PEG blend, MWNTs and PMMA/PEG/MWNTs nanocomposites. The decomposition temperature (onset of inflection) for PMMA/PEG blend is lower than those of its nanocomposites, indicating that the thermal stability of nanocomposites has been improved because of addition of MWNTs. Besides that, the residual weight of PMMA/PEG/MWNTs nanocomposites left increases steadily with the increase of MWNTs loading. As shown in Fig. 6, the weight loss at 345 °C for PMMA/PEG blend is about 85 %, whereas PMMA/PEG/MWNTs nanocomposites are only around 49 - 79 %. This also indicates that the thermal stability of PMMA/PEG blend is significantly improved on incorporation of MWNTs.

Fig. 7 shows the dependence of the decomposition temperature (T_d , 5 % weight loss temperature) on MWNTs content. PMMA/PEG blend and pure MWNTs start to lose weight at 251 °C and 467 °C, respectively. It can be seen that the overall thermal stability of PMMA/PEG/MWNTs nanocomposites, compared with PMMA/PEG blend, is clearly improved; in Fig. 7, the addition of 0.5 wt % MWNTs causes the decomposition temperature of PMMA/PEG blend increase more than 7 °C. The thermal stability of PMMA/PEG/MWNTs nanocomposites may be closely related to following factors: the dispersion state and the loading content of MWNTs.

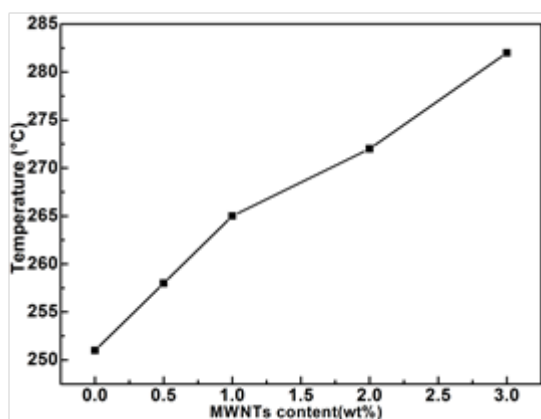


Fig. 7. Decomposition temperature (T_d , 5 % weight loss temperature) as a function of MWNTs loading.

The decomposition temperature of PMMA/PEG/MWNTs nanocomposites increases slightly with increasing MWNTs loading content, probably due to the ease of compact char formation for the nanocomposites during the thermal degradation; more importantly, CNTs is a kind of excellent flame retardant material, which may be ascribed to the following factors: a) high heat conduction ability of CNTs promotes the consumption of heat [37]; b) CNT as electron

acceptor can capture high-energy radicals during the thermal degradation process [38, 39].

On the other hand, high concentration MWNTs would definitely prevent its fine dispersion, and more aggregation or bundles could often be formed because of van der Waals force among the MWNTs, thus deteriorating the thermal stability of the nanocomposites. It is necessary to research the competing effect between the dispersion state and the loading content of MWNTs in depth.

CONCLUSIONS

MWNTs were dispersed into PMMA/PEG blends through ultrasonic assisting with 0.5 %; 1 %; 2 % and 3 % (wt/wt) of MWNTs loadings.

Morphological analysis shows that, at low concentration of MWNTs, it is well dispersed; however, with an increase in MWNTs concentration, it is a nonuniform dispersion, and a large aggregate of MWNTs having a diameter of over 500nm is formed. The POM images of PEG spherulites becomes smaller in the presence of MWNTs; DSC analysis showed that T_m increased very slightly in the PMMA/PEG/MWNTs nanocomposites compared with those in PMMA/PEG blend, and increased with increase of MWNTs concentration. The analysis of thermal degradation in airflow showed a clear improvement of thermal stability for PMMA/PEG/MWNTs nanocomposites, proportionally to MWNTs content.

REFERENCES

1. A. Allaoui, S. Bai, H. M. Cheng, J. B. Bai, *Compos. Sci. Technol.*, **62**, 1993 (2002).
2. S. J. Park, M. S. Cho, S. T. Lim, H. J. Choi, M. S. Jhon, *Macromol. Rapid Comm.*, **24**, 1070 (2003).
3. Y. B. Zou, Y. C. Feng, L. Wang, X. B. Liu, *Carbon*, **42**, 271 (2004).
4. E. N. Konyushenko, J. Stejskal, M. Techova, J. Hradil, J. Kovářová, M. Cieslar, J. Y. Hwang, K. H. Chen, I. Sapurina, *Polymer*, **47**, 5715 (2006).
5. M. K. Yeh, N. H. Tai, J. H. Liu, *Carbon*, **44**, 1 (2006).
6. N. Grossiord, J. Loos, O. Regev, C. E. Koning, *Chem. Mater.*, **18**, 1089 (2006).
7. A. Maity, M. Biswas, *J. Ind. Eng. Chem.*, **12**, 311 (2006).
8. S. T. Kim, J. Y. Lim, B. J. Park, H. J. Choi, *Macromol. Chem. Phys.*, **208**, 514 (2007).
9. F. H. Zhang, R. G. Wang, X. D. He, C. Wang, L. N. Ren, *J. Mater. Sci.*, **44**, 3574 (2009).
10. Y. Wang, R. Cheng, L. Liang, Y. Wang, *Compos. Sci. Technol.*, **65**, 793 (2005).
11. J. C. Kearns, R. L. Shambaugh, *J. Appl. Polym. Sci.*, **86**, 2079 (2002).
12. X. Tong, C. Liu, H. Cheng, H. Zhao, F. Yang, X. Zhang, *J. Appl. Polym. Sci.*, **92**, 3697 (2004).

13. B. Safadi, R. Andrews, E. A. Grulke, *J. Appl. Polym. Sci.*, **84**, 2660 (2002).
14. M. Terrones, *Annu. Rev. Mater. Res.*, **33**, 419 (2003).
15. F. H. Gojny, M. H. G. Wichmann, B. Fiedler, W. Bauhofer, K. Schulte, *Compos. Part A: Appl. S.*, **36**, 1525 (2005).
16. E. T. Thostenson, Z. Ren, T. Chou, *Compos. Sci. Technol.*, **61**, 1899 (2001).
17. H. W. Goh, S. H. Goh, G. Q. Xu, K. P. Pramoda, W. D. Zhang, *Chem. Phys. Lett.*, **379**, 236 (2003).
18. J. N. Coleman, U. Khan, J. Blau, Y. Gun'ko, *Carbon*, **44**, 1624 (2006).
19. H. Ito, T. P. Russell, G. D. Wignall, *Macromolecules*, **20**, 2213 (1987).
20. J. Straka, P. Schmidt, J. Dybal, B. Schneider, J. Spevacek, *Polymer*, **36**, 1147 (1995).
21. X. Lu, R. A. Weiss, *Macromolecules*, **25**, 3242 (1992).
22. H. Schmidt, I. A. Kinloch, A. N. Burgess, A. H. Windle, *Langmuir*, **23**, 5707 (2007).
23. S. Pande, R. B. Mathur, B. P. Singh, T. L. Dhami, *Polym. Compos.*, **30**, 1312 (2009).
24. A. K. Pradhan, S. K. Swain, *J. Mater. Sci. Technol.*, **28**, 391 (2012).
25. G. Gonçalves, S. M. Cruz, A. Ramalho, J. Grácio, P. A. Marques, *Nanoscale*, **4**, 2937 (2012).
26. R. Ormsby, T. McNally, C. Mitchell, N. Dunne, *J Mater Sci Mater Med.*, **21**, 2287 (2010).
27. R. Ormsby, T. McNally, P. O'Hare, G. Burke, C. Mitchell, N. Dunne, *Acta Biomater.*, **8**, 1201 (2012).
28. D. Chen, M. Wang, W. D. Zhang, T. Liu, *J. Appl. Polym. Sci.*, **113**, 644 (2009).
29. G. X. Chen, H. S. Kim, B. H. Park, J. S. Yoon, *Polymer*, **47**, 4760 (2006).
30. S. T. Kim, H. J. Choi, S. M. Hong, *Colloid Polym. Sci.*, **285**, 593 (2007).
31. J. Liu, A. G. Rinzler, H. Dai, J. H. Hafner, R. K. Bradley, P. J. Boul, A. Lu, K. Shelimov, C. B. Huffman, F. Rodriguez-Macias, Y. S. Shon, T. R. Lee, D. T. Colbert, R. E. Smalley, *Science*, **280**, 1253 (1998).
32. S. J. Park, S. T. Lim, M. S. Cho, H. M. Kim, J. Joo, H. J. Choi, *Curr. Appl. Phys.*, **5**, 302 (2005).
33. Y. Zhao, Z. Qiu, W. Yang, *J. Phys. Chem. B*, **112**, 16461 (2008).
34. C. L. Wu, M. Q. Zhang, M. Z. Rong, K. Friedrich, *Compos. Sci. Technol.*, **62**, 1327 (2002).
35. D. N. Bikiaris, A. Vassiliou, E. Pavlidou, P. Karayannidis, *Eur. Polym. J.*, **41**, 1965 (2005).
36. E. Martuscelli, C. Silvestre, C. Glomondi, *Die Makromolekulare Chemie*, **186**, 2161 (1985).
37. J. J. Ge, H. Hou, Q. Li, M. J. Graham, A. Greiner, D. H. Reneker, ... & S. Z. Cheng, *J. Am. Chem. Soc.*, **126**, 15754 (2004).
38. P. C. P. Watts, P. K. Fearon, W. K. Hsu, N. C. Billingham, H. W. Kroto and D. R. M. Walton, *J. Mater. Chem.*, **13**, 491 (2003).
39. M. S. P. Shaffer, A. H. Windle, *Adv. Mater.*, **11**, 937 (1999).

МОРФОЛОГИЯ И ТЕРМИЧНИ ОТНАСЯНИЯ НА НАНОКОМПОЗИТИ ОТ ПОЛИ(МЕТИЛ-МЕТАКРИЛАТ/ПОЛИ(ЕТИЛЕНГЛИКОЛ) С МНОГОСТЕННИ ВЪГЛЕРОДНИ НАНОТРЪБИ

Г. К. Лю

Колеж по материалознание и инженерство, Технологичен университет Хенан, Женгжоу, 450001, Китай

Постъпила на 25 декември, 2013 г.; коригирана на 3 юли, 2015 г.

(Резюме)

Изготвени са многостенни въглеродни нанотръби (MWNTs) с нано-композити от поли(метил-метакрилат/поли(етиленгликол) (PMMA/PEG/MWNTs). Приложена е радикалова обемна полимеризация под действието на ултразвук. Изследван е ефекта на различните процентни натоварвания с MWNTs върху морфологичните и термичните свойства на нанокompозитите от PMMA/PEG/MWNTs. Намерено е, че при ниски концентрации многостенните въглеродни нанотръби се диспергират равномерно в смесите от PMMA/PEG и повишават плътността на зародишообразуване на PEG. Термичният анализ показва, че има ясно изразено подобрене на термичната стабилност на нанокompозитите PMMA/PEG/MWNTs с повишаване на съдържанието на MWNTs.